Third United Nations International Conference on the Peaceful Uses of Atomic Energy

A/CONF.28/P/358
USSR
May 1964
Original: RUSSIAN

Confidential until official release during Conference

NEUTRON PHYSICS PARAMETERS OF SOME WATER-MODERATED URANIUM LATTICES

L.G.Andreev, I.H.Ganev, S.I.Garanin, E.A.Dvoinishnikov, A.I.Dokutchaev, F.S.Drozdov, A.F.Zaitsev, V.P.Katkov, L.V.Komissarov, Ju.N.Knisznikov, Ju.Ja.Kravtchenko, N.A.Lasukov, Ju.V.Nikolski, A.N.Protzenko, G.A.Stoljarov, V.M.Talizin, I.A.Filatjev, Ja.V.Shevelev.

The results are reported of three independent groups of experiments on light water lattices with rod elements. Some of the lattices considered (those incorporating no absorbers) are rather similar to ones described in the publication "Light water lattices", edited by IAEA in 1962, with some differences in enrichment and rod diameters.

In section A the experiments are described on 5% enriched uranium dioxide systems with fuel rod diameters 0.45 cm. Furthermore, binary lattices are considered in this section, including uranium and absorber rods, with optical transparency in the range of 0.75 to 40. The results are reported concerning the critical masses of the lattices and some relations are presented which has been used in calculations.

In Section B the multiplication parameters of the natural uranium dioxide lattices are studied by the method of absorption ratio measurement for core components, the neutron leakage correction being taken into account.

In section C performances of the lattices with magnesium – 2% enriched uranium alloy fuel rods are studied by the pulsed neutron source technique.

This study is performed in Kurchatov Institute of Atomic Energy. The authors of the separate parts of this report are:

Section A – I.H.Ganev, E.A.Dvoinishnikov, A.I.Dokutchaev, A.F.Zaitzev, N.A.Lasukov, A.N.Protzenko.

Section B – S.I.Garanin, V.P.Katkov, Ju.N.Knisznikov, L.V.Komissarov, Ju.Ja.Kravtchenko, Ju.V.Nikolski, G.A.Stoljarov, I.A.Filatjev.

Section C – L.G.Andreev, F.S.Drozdov, V.M.Talizin, Ja.V.Shevelev.

A. CRITICAL EXPERIMENTS WITH LATTICES CONTAINING ABSORBER RODS

One-group method was used in material buckling calculations for binary lattices. Epithermal processes were taken into account by additional factor, introduced into the infinite lattice multiplication constant, according to ref. 1. A considerable reduction in computer time results, which makes possible the precise calculation of the spatial non-uniformity and the time

dependence of the lattice properties due to burnout. The disadvantage factors were calculated in the diffusion approximation, the effective boundary conditions being imposed on the rod surface. A formula was obtained on the basis of consideration of the effective boundary conditions for absorbing cylinder in an infinite non-absorbing medium, realized in ref. 2. This formula does not take into account the scattering in the inner region of the rod and allows the analytical integration when averaging γ over neutron spectra

$$\gamma = fi\,\beta\left(1 - e^{-\frac{f_2}{\beta^2}}\right) + f_3 e^{-\frac{f_4}{\beta^2}} + f_5 e^{-\frac{f_6}{\beta^2}}, \qquad (A-1)$$

where

$$fi = h_1^i + \frac{h_2^i a}{1 + h_3^i a}; \quad a = d\Sigma_t^{env}$$

$$\beta = d\Sigma_c\,(294^oK)\sqrt{\frac{0.0253}{E}}$$

The values of the coefficients h_1, h_2 and h_3 for various i are given below.

i	1	2	3	4	5	6	8	9
h_1	0.7057	0.3	0.5526	0.71	0.1974	5.52	0.8281	0.2367
h_2	0.085	0.243	0.5908	0.32	0.392	0.1765	-1.2934	-0.3069
h_3	2.58	1.337	1.748	1.46	1.2253	0.6044	2.77	2.77

The quantities γ and g_{th} were averaged over the Maxwellian spectrum when imposing the boundary conditions and calculating the self-shielding factor for strong absorber in the thermal region.

The self-shielding factor was calculated from the neutron balance condition, taking into account neutrons, incoming on the rod surface and absorbing in it,

$$g_{th}(E) = \frac{\overline{\phi(r)}}{\phi(r)} = \frac{1}{0.75\,d\,\Sigma_c(E)\overline{\gamma}}. \qquad (A-2)$$

On averaging over the Maxwellian spectrum, we obtain

$$g_{th}\left[\phi(\sqrt{x}) - \frac{2}{\sqrt{\pi}} e^{-x\sqrt{x}}\right] = \frac{1.504}{\beta_o}\left\{f_1 \frac{\sqrt{\pi}}{2}\beta_o\left[1 - \frac{1}{(1+f_2/\beta_o^2)^{3/2}}\right] + \frac{f_3}{(1+f_4/\beta_o^2)^2} + \right.$$

$$\left. + \frac{f_5}{(1+f_6/\beta_o^2)^2}\right\} - \frac{f_1}{\sqrt{\pi}\cdot 0.75}\left[e^{-x}\left(\frac{1+2x}{\sqrt{x}}\right) - e^{-a'x}(a')^{-3/2}\left(\frac{1+2a'x}{\sqrt{a'x}}\right)\right]$$

$$a_1 = 1 + \frac{f_2\lambda}{\beta_o^2}; \quad \lambda = 1.2; \quad x = \frac{E_s}{E_{th}}; \quad \beta_o = \beta(E = E_{th}). \qquad (A-3)$$

358

It was found convenient, in calculating the average self-shielding factor $\bar{g}_e$ for epythermal region, to use the following expression for the quantity γ:

$$\gamma = \frac{f_7 \cdot \beta + f_{10}\beta^2}{1 + f_8\beta + f_9\beta^2} \quad . \qquad (A-4)$$

The coefficients f_8 and f_9 are to be found from the equation for f_i with the above values of h_1, h_2 and h_3; the coefficients f_7 and f_{10} are determined by Eq. (A–5).

$$f_7 = \frac{f_3 + f_5}{2}\ ;\ f_{10} = \frac{2(0.75 - f_7 f_8)}{\sqrt{4f_9 - f_8^2}} \quad . \qquad (A-5)$$

On averaging over the slowing-down neutron spectrum we obtain:

$$\bar{g}_e = \frac{1}{0.75\beta_s}\left[f_7 \ln(1 + f_8\beta_s + \tilde{f}_9\beta_s^2) + \tilde{f}_{10}\left(z + \frac{z^3}{6} + \frac{z^5}{13{,}333}\right)\right] \qquad (A-6)$$

$$\beta_s = \beta_o\sqrt{\frac{E_{th}}{E_s}}\ ;\ z = \frac{y}{\sqrt{1+y^2}}\ ;\ y = \frac{\beta_s\sqrt{4f_9 - f_8^2}}{2 + f_8\beta_5}$$

EXPERIMENTAL ARRANGEMENT AND RESULTS

The core was composed of rod-type fuel elements. The average length of the fuel element tube, filled with sintered uranium dioxide pellets, was equal to 59, 66 cm. Steel- and zirconium-clad fuel elements with the inner diameter of 0.45 cm,were used in the experiments. 5.32% and 5.12% enriched uranium was contained in steel- and zirconium-clad fuel elements, correspondingly. The average weights of the fuel element cores were 76.51 g and 91.63 g, correspondingly. The absorber rods used in the experiments were constructed of steel tube filled with the $B_4C + Al_2O_3$ mixture on the length equal to the core height. The boron content in the boron carbide amounted to 65.6 weight per cent.

In the first series of the experiments "pure" assemblies were studied, containing no boron-filled rods. The rods were arranged in a triangular lattice, the lattice pitch being 7, 8, 14 mm for steel and 8 mm for zirconium-clad fuel elements.

Besides the "homogeneous" assemblies described criticality measurements were made on the assemblies with periodical core heterogeneity.

Some typical lattice cells are illustrated in Fig.A–1 (the boron rods shown in Fig.A–1 were used in the second series of the experiments).

The assemblies were surrounded by practically infinite water reflector (~20 cm.). The water temperature in various assemblies varied in the range of 20±3°C.

The experimental and calculated values of the critical mass for various spacings of "homogeneous" and "heterogeneous" assemblies are listed in Table A–1. The uncertainty

Critical masses of the "pure" assemblies

Table A–I

Fuel element type	Lattice step mm	Lattice cell configuration	$\frac{S_{H_2O}}{S_{UO_2}}$	$\frac{\rho_{II}}{\rho_5}$	G_5^{exp} kg	crit. No. of fuel elements	G_5^{calc} kg
Steel-clad	7	"Homogeneous"	1.53	100	14.0	3937	15.1
	8	"Homogeneous"	2.39	156	7.6	2124	8.1
	8	37–1, no gap	2.49	163	7.2	2030	–
	8	37–7, no gap	3.25	213	5.8	1626	–
	8	37, single row gap	3.52	230	5.6	1589	5.5
	8	37–1, single row gap	3.62	237	5.5	1538	5.5
	8	37–7, single row gap	4.61	301	4.7	1335	4.8
	14	"Homogeneous"	10.06	658	4.7	1319	5.1
Zirconium-clad	8	"Homogeneous"	1.64	98	8.8	2138	–
	8	37–1, no gap	1.73	104	8.1	1974	–
	8	37–7, no gap	2.45	147	5.7	1380	–

Critical number of fuel elements and number of boron rods in two-zone assemblies

Table A–II

No. of experiment	Lattice spacing mm	Central zone			Peripheral zone cell	Number of boron containing cells	Critical number of fuel elements
		Lattice cell	absorber rod				
			boron content g	cladding dia. mm			
1	7	61–1, no gap	7.35	5.[illegible]	"Homogeneous"	28	5641
2	8	37–7, single row gap	7.35	5x4.6	37–7, single row gap	77	3461
3	8	37–7, no gap	0.71	10x8	37–7, no gap	12	2112
4	8	37–7, no gap	1.6	14x12	37–7, no gap	7	2119
5	8	37+11–7	25.6	10x8	37+11–7	19	5394
6	8	37+11–7	57.74	14x12	37+11–7	31	5648
7	8	37+11–7	2.78	10x8	37+11–7	31	5510
8	8	37+11–7	7.42	14x12	37+11–7	54	5636
9	8	37+11–7	1.38	10x8	37+11–7	37	5504
10	8	37+11–7	3.3	14x12	37+11–7	67	5525
11	8	37+11–7	0.71	10x8	37+11–7	46	5522
12	8	37+11–7	1.6	14x12	37+11–7	93	5527

358

of the measured critical mass values is 1.5%. The discrepancy of the experimental and calculated values does not exceed 10%.

In the second series of the experiments two-zone assemblies were studied, containing boron rods in the central zone. Various types of the lattice cells are illustrated in Fig. A–1. The critical assemblies as well as the zones containing boron rods approximate the cylindrical geometry. The results of the criticality measurements of the two-zone assemblies (at T=20°C) are listed in Table A–11.

The calculated and measured values of the material buckling of the absorber rod containing zone are plotted in Fig. A–2 against rod blackness.

The experimental data are in good agreement with the calculated values, thus giving ground to use the above relatively simple technique in a rather wide range of ρ_H/ρ_5 and $d\Sigma_c$ values for the boron rods.

B. EXPERIMENTAL DETERMINING PARAMETERS OF NATURAL URANIUM DIOXIDE LATTICES

1. PHYSICAL PARAMETERS OF THE LATTICE

The definitions of neutron maltiplication and slowing-down parameters used in this paper do not imply the subdivision of neutron spectra into parts and are similar to those of ref. 3. The parameters studied were determined experimentally using the technique described in the same paper. Furthermore, the corrections for neutron leakage were introduced in the one-group approximation. Used in the correction calculations migration areas from generation neutrons in U^{235} to fission in U^{238} with taking into account cascade multiplication (M_8^{f2}.) and absorption due to main U^{238} resonances (M_8^{R2}) were determined from poisoning experiments, with boric acid solution. It is possible to express M_8^{f2} in terms of the neutron absorption ratio for poisoned and non-poisoned systems, on the assumption, that poisoning does not change the neutron spectrum in the above resonance region:

$$(M_8^f)^2 = \frac{\left(\frac{\Pi_8^f}{\Pi_5^f}\right)_{pois} \Big/ \left(\frac{\Pi_8^f}{\Pi_5^f}\right)_{pure}}{B^2_{pure} - B^2_{pois}\left(\frac{\Pi_s^f}{\Pi_5^f}\right)_{pois} \Big/ \left(\frac{\Pi_8^f}{\Pi_5^f}\right)_{pure}}, \qquad (B-1)$$

where B^2 is buckling, Π_8^f and Π_5^f are numbers of capture events, followed by U^{238} and U^{235} fission, correspondingly. M_8^{R2} is determined similarly.

The data obtained from poisoning experiments make it possible to determine M^2 and to evaluate the form of the critical equation.

358

Let:
$$B^2(C_B) = -A\,[1 - e^{(C_o - C_B)l}]\ ; \qquad (B-2)$$

$$\ln K_\infty = (C_o - C_B)m\ , \qquad (B-3)$$

where C_B is the boron concentration.

The coefficients A, C_o, l and m are to be determined from the experimental data. Taking into account, that

$$M^2 = \frac{\partial K_\infty^{-1}}{\partial C_B}\bigg|_{B^2=0} \quad \frac{\partial C_B}{\partial B^2}\bigg|_{B^2=0} = \frac{m}{lA} \qquad (B-4)$$

the critical equation can be rewritten as:

$$(1 + \frac{B^2 M^2}{n})^n = K_\infty \qquad (B-5)$$

Here $n = \frac{m}{l}$

2. EXPERIMENTAL EQUIPMENT

Two research reactors were used in the experiments. The first one was designed to measure the following parameters: K_∞, μ, ϕ, θ, ν_{eff}, P and σ_9^f / σ_5^f. It was a critical assembly, comprising the central "seed" zone and the lattices investigated around it. The triangular lattices under study were assembled from fuel elements with spacings of 13, 15, 17 and 19 mm. The elements used were fabricated from aluminium tubes and filled with natural uranium dioxide pellets of 8.0 g/cm^3 density to a height of 1200 mm. The outer tube diameter was 11.3 mm, the wall thickness 0.7 mm, the pellet diameter 9.4 mm.

The other research reactor was used to measure B^2, M^2, $(M_8^f)^2$, and to evaluate the form of the critical equation for 13 mm spacing lattice. It had a form of a hollow cylinder with a hexagonal tank in the central region containing the lattice under study. The arrangement described made it possible to poison the lattice by the boric acid solution and to conduct the experiments on a dry lattice (without water in the tank).

3. RESULTS

The results of the measurements of the lattice parameters are presented in Table B–1 and in Fig. B–1 (See Table B–II for designations).

The reactor of hollow cylindrical geometry has been used for the experiments with 13 mm spacing lattice, both dry and poisoned with boric acid. On the assumption of M_8^{f2} / M^2 value being in the region from 0.6–0.9 for dry lattice (for boron-free lattice imbedded in water the above ratio was found to be 0.4), the following data have been obtained for dry system:

$$\Pi_8^f / \Pi_5^f = 0.60 \pm 0.08; \quad K_\infty = 0.22 - 0.25; \qquad \mu = 1.14 - 1.25$$

$$(M_8^f)^2 / M^2 = 0.6 - 0.9; \quad P = 0.8 \pm 0.3; \qquad \alpha_5^f = 0.48 \pm 0.02$$

The above values are to be regarded as preliminary estimates and are subject to more accurate definition.

The results for 13 mm spacing boron-poisoned lattice are listed in Table B–II.

As an analysis of the experimental data has shown, the $B^2(C_B)$ and $K_\infty(C_B)$ variations can well be described by Eqs. (B–2) and (B–3) with the following values of the coefficients:

$$A = 130 \cdot 10^{-4}; \quad C_o = -0.5; \quad l = 0.294; \quad m = 0.296.$$

From the data obtained one can find $M^2 = 77.0 \pm 3$ cm^2; $n = 1.0 \pm 0.01$.

As it will be seen from the above results, the lattice under study can be described by the one-group critical equation within the limits of the experimental errors.

4. COMPARISON OF EXPERIMENTAL RESULTS WITH CALCULATIONS

Commonly used scheme was applied for the calculations of the lattice neutron multiplication parameters; however, the values presented have the meaning adopted in this work.

As the transparencies of the lattices investigated for fission neutrons are very high, it is possible to calculate μ from the formula for homogeneous mixture making use of the published data on effective cross sections (See ref. 4).

The values of μ thus obtained are in satisfactory agreement with the experimental data (See Fig. B–1), but for 13 mm spacing lattice, where a substantial discrepancy is observed.

When evaluating ϕ, equation (53.18) of ref. 2 has been used for the calculation of resonance integral.

According to the results of the analysis of available experimental data on resonance capture in uranium dioxide blocks, the numerical values of the coefficients of the volume and surface terms were assumed to be 10.4 and 31.25, correspondingly (the $1/v$ part of the cross-section being neglected).

The calculated values of ϕ are in good agreement with the experimental data for all spacings.

The quantities ν_{eff} and θ have been calculated with the use of Wilkins equation. The Wilkins distribution was assumed for neutron energies up to 0.5 ev, while at higher energies the spectrum was supposed to be Fermian slope. The effective cross sections were obtained by averaging over the above spectrum, the screening effects, dependent on lattice geometry and neutron energy being taken into account.

The procedure described yielded the values of ν_{eff}, which are not quite in satisfactory agreement with the experiment, the better agreement being observed for θ.

The calculated values of neutron multiplication parameters are shown in Fig. B–1.

Measured values of lattice parameters

Table B–I

Parameter \ Lattice spacing, mm	13	15	17	19
Π_8^f / Π_5^f *	0.133±0.008	0.075±0.005 0.076±0.004	0.051±0.004 0.052±0.003	0.044±0.003 0.042±0.003
Π_5 / Π_5^f	1.225±0.010	1.209±0.009	1.202±0.010	1.198±0.010
Π_8^r / Π_5^f	1.611±0.050	1.238±0.004	1.100±0.040	0.983±0.035
Π_H / Π_5^f	0.222±0.009	0.474±0.012	0.728±0.018	1.010±0.025
Π_{Al} / Π_5^f	0.067±0.004	0.067±0.003	0.067±0.003	0.066±0.003
$\Pi_8^{1/\nu} / \Pi_5^f$	0.702±0.015	0.687±0.013	0.681±0.013	0.678±0.011
a_8^r	0.61±0.03	0.47±0.02	0.39±0.02	0.340±0.025
a_ν	0.11±0.01	–	–	–
a_5^f	0.105±0.003	0.058±0.003	0.040±0.003	0.028±0.003
a_9^f	0.080±0.003	0.04	0.03	0.02
a_e^f	–	0.140±0.001	0.100±0.002	0.081±0.001
K_∞	0.876±0.025	0.878±0.020	0.836±0.015	0.788±0.017
$\mu-1$	0.109±0.008	0.063±0.004	0.045±0.002	0.038±0.002
ϕ	0.709±0.020	0.815±0.015	0.865±0.015	0.906±0.018
θ	0.870±0.005	0.778±0.006	0.703±0.009	0.658±0.010
ν_{eff}	1.282±0.020	1.303±0.025	1.312±0.017	1.317±0.020
P	1.32±0.04	1.022±0.025	0.914±0.020	0.818±0.020
$\beta_{9/5} = \frac{(\sigma_9^f / \sigma_5^f)_{\text{lattice}}}{(\sigma_9^f / \sigma_5^f)_{\text{Maxwell}}}$	1.29±0.02	1.17±0.02	1.12±0.01	1.07±0.01
$\bar{n}_{H_2O} / \bar{n}_u$	1.063±0.030	1.12±0.03	1.11±0.03	1.10±0.03

* The values of Π_8^f/Π_5^f in the first line of the table were obtained in the experiments with depleted and natural uranium as indicators, the second line contains the values, obtained from cadmium ratio measurements on natural uranium and U^{235} $(\frac{\Pi_8^f}{\Pi_5^f} = \frac{a_e^f - a_5^f}{1 - a_e^f})$.

All the data listed in the table are obtained on averaging the results of two experimental groups.

358

Poisoned lattice parameters (13 mm spacing)

Table B–Ii

Parameter \ H_3BO_3 concentration mg/ml	0.0	3.96	6.35	10.80	14.70
Π_8^f / Π_5^f	0.133±0.008	–	–	0.149±0.010	–
Π_5 / Π_5^f	1.225±0.010	–	1.230±0.005	1.235±0.005	–
Π_8^r / Π_5^f	1.611±0.050	–	1.91±0.03	2.15±0.03	–
Π_{Al} / Π_5^f	0.067±0.004	–	0.066±0.005	0.068±0.005	–
Π_H / Π_5^f	0.222±0.008	–	0.226±0.009	0.231±0.009	–
Π_B / Π_5^f	0	–	0.43±0.01	0.73±0.01	–
α_8^r	0.61±0.03	–	0.65±0.02	0.68±0.02	–
α_v	0.11±0.01	–	0.13±0.01	0.17±0.01	–
α_5^f	0.105±0.003	–	0.09±0.01	0.10±0.01	–
α_9^f	0.080±0.003	–	–	–	–
K_∞	0.875±0.025	–	0.707±0.010	0.623±0.010	–
$\mu-1$	0.109±0.008	–	–	0.101±0.008	–
ϕ	0.709±0.020	–	0.700±0.008	0.692±0.008	–
θ	0.870±0.005	–	0.727±0.010	0.653±0.010	–
ν_{eff}	1.282±0.020	–	1.26±0.01	1.25±0.01	–
P	1.32±0.040	–	1.55±0.02	1.73±0.03	–
$(M_8^f)^2$ (cm^2)	33±5	–	–	–	–
$(M_8^R)^2$ (cm^2)	80±5	–	–	–	–
$B^2 \cdot 10^4$(cm^{-2})	16.8±0.06	30.7±0.05	37.5±0.08	47.4±0.16	53.3±0.14

Here Π_i/Π_j is neutron absorption ratio for i and j–th components of the lattice;

α_i – is the share of i–th component in epycadmium neutron absorption.

Indices "8", "5", "Al", "H", "B" refer to U^{238}, U^{235}, Al, H and B in the core, indices f, r, R designate fission, radiative capture and resonance absorption on U^{238}, correspondingly; α_v and α_9^f are cadmium ratioes for V^{51} and Pu^{239}.

358

C. LATTICE PARAMETER STUDY BY PULSED NEUTRON SOURCE TECHNIQUE

A common method of studying the properties of neutron multiplication systems implies the measurement of stationary neutron density distributions obtained in critical experiments or on subcritical systems due to constant neutron source. In many instances, however, more precise results can be obtained in a simplier way by studying non-stationary distributions, produced by initial neutron pulse. The quantity measured directly in this circumstances is the time constant of neutron density decay at a given point in the system. Even more effective are the experiments, employing both the methods simultaneously.

Both in planning the experiments with a pulsed neutron source and treating the obtained results the approximate relations are of use given below, describing space-time distribution of neutron flux. The amplitude of the spatial harmonic $\psi_n(\vec{n})$ associated with buckling B_n^2 in an interval between two pulses varies according to the relation:

$$\phi_n(t) \sim \exp\left(S_{no}t\right) + \frac{1}{\rho_n S_{no} r} - \epsilon_n \frac{t}{r}, \qquad \text{(C–1)}$$

where ρ_n is reactivity (expressed in terms of β_{eff}) corresponding to n – th harmonic, i.e.

$$\rho_n = \frac{1 - [K_\infty \tilde{f}(B_n^2)]^{-1}}{\beta_{eff}} = \frac{1 - \tilde{f}(B_{o\,cr}^2)/\tilde{f}(B_n^2)}{\beta_{eff}}. \qquad \text{(C–2)}$$

The function $\tilde{f}(B^2)$ is the leakage escape probability i.e. Fourier transform of the second neutron generation sources distribution for point primary source in infinite media. If $K_\infty - 1 > \beta_{eff}$ then ρ_n is large and negative, when $n \neq 0$.
The parameter ϵ_n

$$\epsilon_n = \frac{\bar{\lambda}\, T}{\beta_{eff}} \cdot \frac{\tilde{f}(B_{o\,cr}^2)/\tilde{f}(B_n^2)}{(1-\beta_n)^2} \qquad \text{(C–3)}$$

is very small, since the first co-factor is very small ($\bar{\lambda} = \sum_i \frac{\beta_i}{\beta} \lambda_i$ is the mean value of the decay constant for delayed neutron sources, T is the prompt neutron life time), and the second co-factor in any case does not exceed unity. $B_{o\,cr}^2$ designates the B_o^2 value for a system of critical dimensions. We have for S_{no}:

$$-S_{no} = \frac{(1-\rho_u)\beta}{r} \cdot \frac{\tilde{f}(B_n^2)}{\tilde{f}(B_{o\,cr}^2)}(1+\epsilon_n) = \frac{1-\rho_n}{1-\beta_{eff}\rho_n} \cdot \frac{\beta_{eff}}{r}(1+\epsilon_n). \qquad \text{(C–4)}$$

The interval r between two pulses is supposed to satisfy the following inequalities:

$$|S_{no}|\, r \gg 1; \qquad \bar{\lambda}\, r \ll 1 \qquad \text{(C–5)}$$

both being possible to hold simultaneously, since $\bar{\lambda}/|S_{no}|$ similarly to ϵ_n is very small.

As it follows from Eq. (C–1) and inequalities (C–5), neutron flux $\phi(t)$ can be regarded as a sum of rapidly varying part and "background". In turn, the background is a sum of a constant and approximately linearly decaying term. The total background variation is only a small part of the rapidly varying component, of the order of $\bar{\lambda} T / \beta_{eff}$. The background-to-rapid component ratio depends upon the degree of the system subcriticality and the pulse repetition frequency. When $|S_{oo}|$ is supposed to be large and constant, it follows, that the background increases in inverse proportion to ρ_o (being lower for $n > 0$ harmonics). The background to the most slow exponent amplitude [i.e. $\exp(S_{oo}t)$] ratio for critical system increases after each pulse, the increment being $T / \beta_{eff} \bar{r}$, where $\bar{r} = \sum_i \frac{\beta_i}{\beta} \lambda_i^{-1}$. When the number of pulses totals to $\beta_{eff} \frac{\bar{r}}{T}$ or at a high pulse repetition rate even before (when a total number of pulses $\beta_{eff}/\bar{\lambda} T$ is attained), the background becomes equal to the initial value of the rapid component, and the system is to be shut down for a long time. With $|\rho_o| \sim 1$ the rapid component already can be separated easily from the background. The main exponent $\exp(S_{oo}t)$ begins to dominate after a short time, since for nearly critical system

$$\frac{S_{no}}{S_{oo}} = \frac{1 - \rho_n}{1 - \rho_o} \cdot \frac{\tilde{f}(B_n^2)}{\tilde{f}(B_o^2)} \gg 1 . \qquad (C–6)$$

The increase of higher harmonic contribution in strongly subcritical system makes it difficult to measure the quantity S_{oo}. When $|\rho_o| \gg 1$ we obtain, instead of Eq. (C–6):

$$\frac{S_{no}}{S_{oo}} = \frac{1 - \tilde{f}(B_n^2)/\tilde{f}(B_{o\,cr}^2)}{1 - \tilde{f}(B_o^2)/\tilde{f}(B_{o\,cr}^2)} . \qquad (C–7)$$

In the limit $B_o^2 \to 0$ the above ratio becomes unity. Without having resource to the special methods of the source-detector disposition, it is possible to determine S_{oo} at $\tilde{f}(B_o^2) \geq ½$.

The measurement of the S_{oo} versus system dimensions (B^2) dependence makes possible the determination of important media parameters. E.g., near-critical experiments yield a quantity

$$-S_{oo\,cr} = \frac{\beta_{eff\,cr}}{T} , \qquad (C–8)$$

the measurements, performed in a wide interval of B^2 values offer the possibility to determine the forms of the functions $\tilde{f}(B^2)$ and K_∞. Extrapolation of $\tilde{f}(B^2)$ to $B^2 = 0$ yields

$$K_\infty = 1 - \beta_{eff} \frac{S_{oo}(0)}{S_{oo}(B_{cr}^2)} ; \qquad (C–9)$$

$$M^2 = \frac{\beta_{eff}}{K_\infty} \cdot \frac{(dS_{oo}/dB^2)_{B^2=0}}{S_{oo}(B_{cr}^2)} . \qquad (C–10)$$

356

The above relations imply that the time of birth of any next generation neutron and its distance from the source are not correlated statistically. This assumption is well satisfied in water-moderated uranium systems, since the neutron migration is small ($L^2 \ll M^2$) in this case in the energy interval of significant absorption. Furthermore the dependence of β_{eff} on system dimensions has not been taken into account. The corresponding corrections are found to be very small.

The following relation can be obtained for zeroth harmonic:

$$[1 - \beta_{eff}(B_o^2)]K_\infty \tilde{f}(B_o^2) = 1 - \beta_{eff}(B_{o\,cr}^2)\frac{S_{oo}(B^2)}{S_{oo}(B_{cr}^2)}(1+F+G+H+J). \qquad (C-11)$$

Here F, G, H, J are corrections for thermal neutron diffusion, capture during slowing down and thermalization, deviation of the capture Σ_c and fission Σ_f cross sections from $1/v$ law, and blocking-effect, correspondingly. When $L^2 \ll M^2$, we obtain

$$F = (1 - \frac{B_o^2}{B_{o\,cr}^2})B_{o\,cr}^2 L_\infty^2 ; \quad L_\infty^2 = D_\infty T_\infty \qquad (C-12)$$

(the infinity index refers to the neutrons in thermal equilibrium with media).

$$G = F\int_o^\infty t\,\delta D(t)\frac{dt}{D_\infty T_\infty^2} ; \quad \delta D = D(t) - D_\infty . \qquad (C-13)$$

Here D(t) is diffusion coefficient averaged over neutron spectra which forms at a time t after neutron birth

$$H = H_{epith} + H_{th} \approx -(\frac{S_{oo}}{S_{oo\,cr}} - 1)\beta_{eff}\int_o^\infty \frac{\delta(\Sigma_f v)}{(\Sigma_f v)_\infty}\frac{dt}{T_\infty} ; \qquad (C-14)$$

$$\delta(\Sigma_f v) = (\Sigma_f v)_t - (\Sigma_f v)_\infty .$$

In particular, the epithermal contribution to H is determined by

$$H_{epith} \approx (1 - \frac{S_{oo}}{S_{oo\,cr}})\beta_{eff}\frac{\bar{J}_f}{\bar{\xi}\bar{\Sigma}_s}\cdot\frac{\overline{\Sigma_a v}}{\overline{\Sigma_f v}} ; \quad \bar{J}_f = \int_{0.1\,ev}^\infty [\Sigma_f(E) - \Sigma_f(kT)\sqrt{\frac{kT}{E}}]\frac{dE}{E} . \qquad (C-15)$$

The heterogeneity correction can be evaluated approximately from the following formula:

$$J = (S_{oo} - S_{oo\,cr})r;$$

$$r = (1 - \frac{\phi_f}{\phi_m})T_f \frac{T_m(1-\theta)}{T_m(1-\theta) + T_f[\theta + (1+\phi_f/\phi_m)(1-\theta)]} , \qquad (C-16)$$

358

where T_f, T_m are the life times of neutrons in fuel rod and moderator, ϕ_f, ϕ_m are corresponding fluxes and θ is neutron absorption probability in rod.

In buckling (B^2) calculations it is important to take into account the extrapolation distance (δ) dependence on the core boundary curvature. Furthermore, δ is influenced by the non-stationary character of the process itself and the value of $S_{oo} = \alpha$. In fact, the non-stationary equation with exponential decay is an equivalent of stationary equation with the effective capture cross section

$$\Sigma_{eff} = \Sigma - \frac{\alpha}{v} \cdot \qquad (C-17)$$

However, δ is dependent on the capture cross section. Thus, decrease in Σ_{eff}, obviously, would result in increase of δ. The physical explanation of this fact follows from the considerations given below. The neutrons, diffusing in the reflector core at any time, have arisen some time ago, when the neutron density in the core was higher than presently existing. Hence, the core reflux to leakage ratio at any time is higher than in stationary conditions. That is, the reflector efficiency during the neutron density decay is higher than in stationary conditions.

Cadmium shielding of core is a radical method of decreasing variations of δ. Then the reflector efficiency is determined by fast neutron reflux only, i.e. it does not depend on the effective capture cross sections and, hence, on α. The dependence of δ on the core boundary curvature radius was proved to be weak if the core and reflector diffusion coefficients are approximately equal.

Without resorting to stationary neutron distribution measurement, the values of δ and the dependence of this quantity on core boundary curvature seem possible to be determined from experimental α vs. B^2 curves, obtained for a wide range of variation of the factors δ depends upon. For example, comparison of B^2 values obtained for cylindrical cores of different height and radius but characterized by the same value of α offers the possibility, in principle, to determine extrapolation distance.

The authors have studied water-moderated uranium system, containing 2% enriched uranium–magnesium alloy rods arranged in triangular lattice of 60 mm spacing. Neutron source and a thermal neutron detector were located in the core. The zirconium tritide target (8 mm dia.) of the neutron generator was used as a neutron source. A scintillation counter with Li^6F + ZnS powder, pressed on the organic glass light pipe butt-end was employed as a suitable detector satisfying main requirements: minimum neutron field perturbation and high sensitivity to neutrons combined with good neutron- γ-ray discrimination.

The measurements of thermal neutron density time dependence have been performed for 12 core configurations differing in number of fuel channels and height, though all the assemblies being nearly cylindrical in shape. The thermal neutron density time decay constant α was measured versus buckling B^2 for assemblies of two types: 1) cadmium shield-free assemblies surrounded by water reflector, 2) cadmium shielded assemblies, i.e. ones separated from reflector by cadmium sheet. The cadmium sheet clinged to the core tightly, reproducing elementary cell configuration on the core boundary. Specifical positioning of the source (at the core center) and detector (at 2/3 of core height and 0.44 of radius produced the most

358

favorable conditions for singling out the fundamental mode in neutron distribution (See Fig. C–1).

The values of the axial (δ_H) and radial (δ_r) extrapolation distances were determined from radial and axial neutron flux distributions measured with indium foils in critical assembly. The radial flux distributions have been measured along five radii in the central plane.

To prove a weak dependence of the decay constant α on the deviation of the core from cylindrical shape check experiments have been performed on one of the assemblies with a small number of fuel channels. The deviations substantially exceeding those inherent in the parameter measurements were found to produce no significant changes in α. Hence, the use can be considered for buckling calculations of the following ideal cylinder formula:

$$B^2 = \frac{2.405}{R + \delta_r} + A\left(\frac{\pi}{H + 2\delta_H}\right)^2, \qquad (C-18)$$

where $A = M_H^2 / M_r^2$ is the migration area anisotropy ratio.

A comparison of the family of curves $\alpha = f(B^2)$ obtained for core configurations of the same radii to those corresponding to different radii made it possible to determine anisotropy ratio A and dependence of δ_r on core boundary curvature radius. For given values of δ_H and δ_{r0} (δ_{r0} is δ_r value for critical assembly) the above curves can be matched at definite A values and definite form of $\delta_r = f(r)$ only, the deviations of the curves due to these two factors displaying different behaviour and being sensitive to the change of A and $\delta_r = f(r)$. The curve matching at the values of δ_H and δ_{r0} obtained experimentally yields A = 1.1 and displays no dependence of δ_r on boundary curvature. The following good approximations were found by the least square method under these conditions: for assemblies surrounded by water

$$\alpha = -1954 + 706000\ B^2 - 21400000\ B^4, \qquad (C-19)$$

for cadmium shielded assemblies

$$\alpha = -1928 + 664000\ B^2 - 11400000\ B^4 \qquad (C-20)$$

illustrated in Fig. C–2. The difference between Eqs. (C–19) and (C–20) could possibly be attributed to the influence of the non-stationary character of the process on extrapolation distance in the cadmium-free assemblies. The difference decreases with the increase of core dimensions (the influence of the non-stationary nature of the process becomes less significant as α decreases). The Eqs. (C–19) and (C–20) yield nearly equal values of α_{cr}

According to the three group calculations δ_r does not depend on the boundary curvature radius for cadmium-free and cadmium shielded assemblies. The calculated extrapolation distance for cadmium – free assemblies coincides with the experimental value, whereas for cadmium shielded assemblies it lies higher. The maximum difference between measured and calculated buckling values, the latter including the calculated correction for non-stationarity, amounts to 1%. The corrections for thermal neutron diffusion, capture during thermalization and diffusion, deviation of the cross sections Σ_a and Σ_f from $1/v$ law and blocking-effect, are insignificant (1%) and of different signs.

The parameters of the described water moderated uranium system determined in the present work, are listed below.

1. Critical load at 22°C (core height 80 cm)

   N_{cr} = (204.9±0.2) fuel elements

2. Material buckling

   $B^2_{cr} = 3.229 \cdot 10^{-13}$ cm^{-2}

3. Buckling for prompt criticality conditions

   $B^2_{prompt} = 3.02 \cdot 10^{-3}$ cm^{-2}

4. Radial extrapolation distance

   δ_r = (7.0±0.3) cm.

5. Axial extrapolation distance

   δ_H = (8.5±0.3) cm.

6. Infinite media multiplication constant

   K_∞ = 1.14±0.01

7. Mean prompt neutron life time

   $T = (70 \pm 4) \cdot 10^{-6}$ sec.

8. Migration area for radial direction

   $M^2_r = (41 \pm 2)$ cm^2

9. Migration area for axial direction

   $M^2_H = (45 \pm 2)$ cm^2

10. Migration area anisotropy ratio

    A = 1.10±0.01

11. Effective fraction of delayed neutrons

    β_{eff} = 0.0072±0.0003

12. Temperature coefficient of reactivity

    $\left.\frac{\Delta \rho}{\Delta T}\right|_{22^oC} = 1.5 \cdot 10^{-4}$ (degree)$^{-1}$

The pulse-source method has some advantages which secure its success in the study of uranium-water systems.

1. Measurement of the relation of $\alpha(B^2)$ within a rather wide range of the variation of B^2 and a very high accuracy of experimental value of α permit to determine a complex of the parameters K_∞, M^2, T with reliability and high accuracy.

2. The assurance of the results produced is increased due to the absence of substantial corrections. The only significant correction on the variability of the process is important in the calculation of the highest moments of $\tilde{f}(B^2)$ — function.

3. The precision of the results is determined particularly by the precision of the effective fraction β_{ef} of delayed neutrons and by the precision of the effective reflector addition δ.

358

This method provides with the principal possibility of the determination of δ.

4. The pulse-source method provides the more sensitive way of determination of the coefficient of anisotropy for the migration area $A = \frac{M_H^2}{M_r^2}$ and of the dependence of the effective addition on curve-radius of the boundary.

5. The measurements with the calibrated instruments are simple and safe, they take rather little time since one deals with highly subcritical assemblies. These factors are substantial particularly in the examination of the series of lattices.

6. The method permits to define the highest function-moments $\tilde{f}(B^2)$. For this purpose it is essential to eliminate the correction effect on the variability and to reduce the effect of δ on the value of the geometrical parameter. It is practicable for the bare homogeneous systems.

7. The pulse-source method can be used in the estimation of the critical dimensions for the instantaneous neutrons by the measurement of $\alpha = f(B^2)$ for the assemblies with the critical mass of 0.1–0.3, with the extrapolation of the dependence found of

$$\alpha = f(B^2) \text{ to the point } \alpha = 0.$$

REFERENCES

1. *Б.Л.Иоффе, Л.Б.Окунь.*"Атомная энергия", 1 (1956), №4, стр.80.
2. *Г.И.Марчук.*"Числовые методы в расчетах ядерных реакторов", Атомиздат, 1958 г.
3. *S.M.Feinberg* et al. "Fuel Burnout for Water-Moderated Water-Cooled Power Reactors and Uranium-Water Lattice Experiments. Second Geneva Conference on Peaceful Uses of Atomic Energy. Report №2145, v. 13,p.348 (1958).
4. *A.Sauer.* Nucleonics, 5, 3,S.110, April 1963.

358

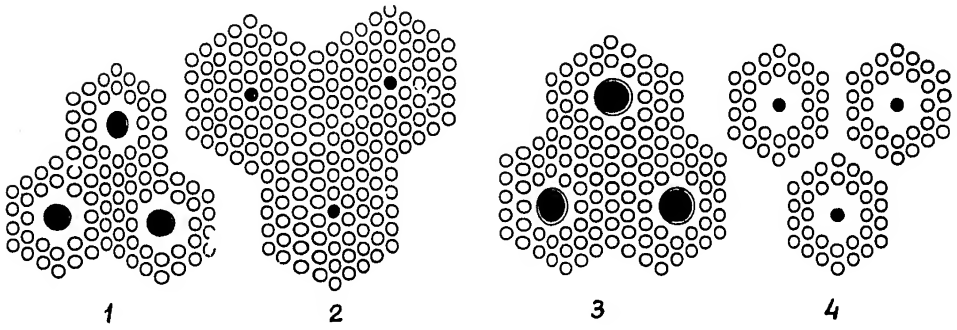

FIG.A–1. TYPICAL CELL CONFIGURATIONS. 1. (37–7) GAPLESS CELL. (61–1) GAPLESS CELL. 3. (37+II-7) CELL. 4. (37–7) CELL WITH SINGLE ROW GAP

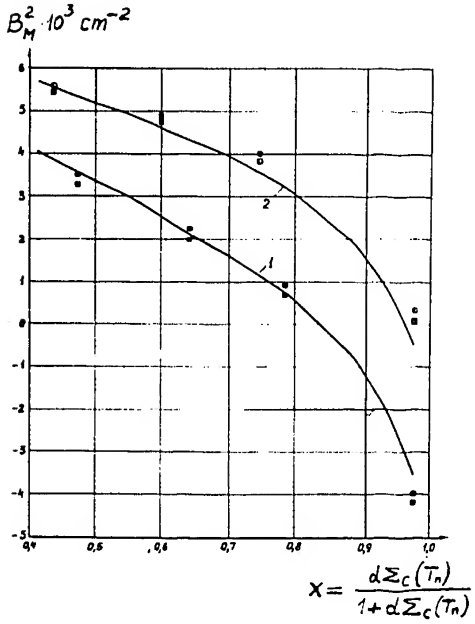

FIG.A–2. MATERIAL BUCKLING vs. BORON ROD BLACKNESS. STEEL CLAD FUEL ELEMENTS, 8 MM SPACING, (37-7+II) CELL. 1. CALCULATED RESULTS FOR 14x12MM DIA. RODS. 2. CALCULATED RESULTS FOR 10x8 MM DIA. RODS ●, ⊙ – EXPERIMENTAL VALUES BASED ON TWO-GROUP CRITICAL EQUATION FOR TWO-ZONE REACTOR WITH RODS OF 14x12 MM DIA. AND 10x8 MM DIA., CORRESPONDINGLY. ■, ⊡ – AS ABOVE, BASED ON ONE GROUP APPROXIMATION.

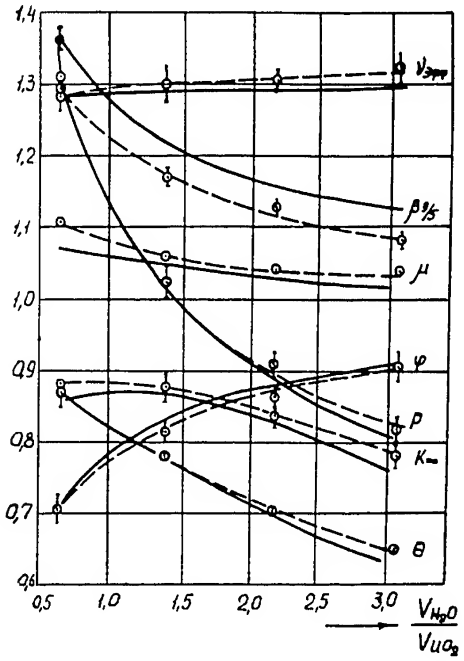

FIG.B–1. PARAMETERS OF THE LATTICES STUDIED vs. WATER TO URANIUM DIOXIDE VOLUME RATIO V_{H_2O}/V_{UO_2} – – – – – – – – EXPERIMENTAL CURVE; —— – CALCULATED CURVE

35e

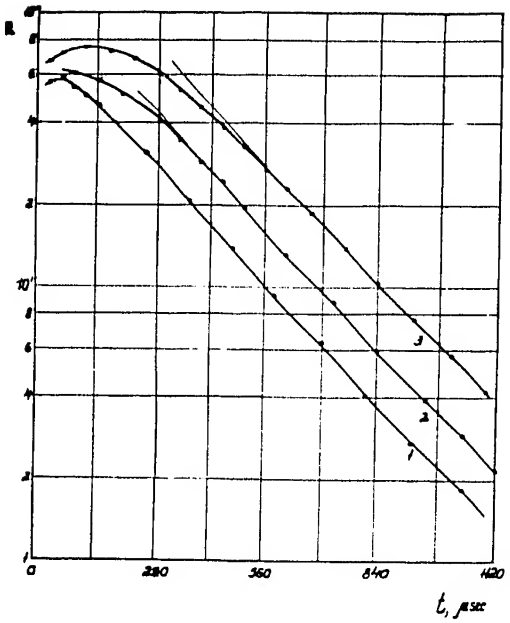

FIG.C–1. HIGHER HARMONIC CONTRIBUTION FOR VARIOUS SOURCE AND DETECTOR POSITIONS (r_s, z_s ARE SOURCE COORDINATES; r_d, z_d ARE DETECTOR COORDINATES).

CURVE 1. $r_s = 0$; $Z_s = 0.5H$; $r_d = 0.54$ R; $Z_d = \frac{2}{3}H$. CURVE 2. $r_s = 0$; $Z_s = 0.5$ H; $r_d = 0.54R$; $Z_d = 0.8H$.

CURVE 3. $r_s = 0.44R$; $Z_s = 0.5H$; $r_d = 0.54R$; $Z_d = \frac{2}{3}$ H.

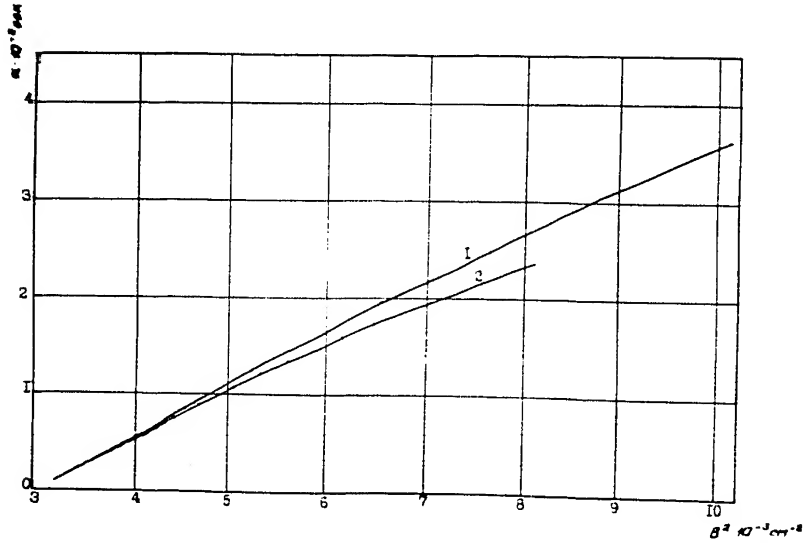

FIG.C–2. THERMAL NEUTRON DENSITY DECAY CONSTANT vs. BUCKLING. CURVE 1. CADMIUM SHIELDED ASSEMBLIES, Eq.(C–20). CURVE 2. ASSEMBLIES SURROUNDED BY WATER REFLECTOR, Eq.(C–19).

558